(Proof version)

Cellular dynamo in a rotating spherical shell

A.V. GETLING[1], R.D. SIMITEV[2,★], and F.H. BUSSE[2]

[1] Institute of Nuclear Physics, Lomonosov Moscow State University, 119992 Moscow, Russia
[2] Institute of Physics, University of Bayreuth, 95440 Bayreuth, Germany

Abstract. Magnetoconvection in a rotating spherical shell is simulated numerically using a code developed by Tilgner and Busse. The thermal stratification is convectively unstable in the outer part and stable in the inner part of the shell. Regimes are found in which the convective flow is weakly affected by rotation and preserves its cellular structure. The dipolar component of the large-scale magnetic field exhibits undamped oscillations. It appears that convection cells slightly modified by rotation can be building blocks of the global dynamo. The generation of the magnetic field is thus due to regular "macroscopic" flows, and their structure itself may ensure the presence of the α effect responsible for the action of the dynamo. Such dynamos can be called deterministic, in contrast to those in which the maintenance of the magnetic field is related to the statistical predominance of a certain sign of helicity in the turbulent velocity field. Investigation of conditions under which dynamos of this sort can operate could suggest a more definite answer to the question of the origin of solar and stellar magnetic fields.

1. Introduction

Intimate interrelation and interdependence between the local and global magnetic fields on the Sun can hardly be a debatable point. Although mean-field electrodynamics proved to be a very efficient tool to investigate global dynamos of the Sun and stars, this important feature falls beyond the scope of the mean-field theories. To comprehend the physical mechanisms of the interplay between the local and global processes, one needs to use a detailed, "deterministic" description of the structural elements present in the flow and magnetic field instead of considering the statistical predominance of one sign of velocity-field helicity or another.

The idea that the connecting link between magnetic fields widely differing in spatial scale may be convection cells in the solar subphotospheric zone, so that a cell *locally* interacting with the magnetic field can serve as a building block of the *global* dynamo, was put forward as long ago as in the mid-1960s. Tverskoy (1966) represented the convection cell by a toroidal eddy and demonstrated, in the framework of a kinematic approach, that such a model convection cell can amplify the magnetic field and produce characteristic bipolar magnetic configurations. This approach was also used by Getling & Tverskoy (1971) to construct a model of the global dynamo in which toroidal eddies distributed over a spherical shell, acting jointly with the differential rotation of the shell, maintain a sign-alternating global magnetic field. If a poloidal magnetic field is present, the differential rotation produces a toroidal component of the global magnetic field. If the local magnetic configuration produced by an eddy interacting with the large-scale toroidal field is rotated by some angle about the axis of the eddy, this configuration contributes to the regeneration of the poloidal component of the global magnetic field. The rotation of the local magnetic-field pattern can be expected if the system rotates as a whole and the flow is affected by the Coriolis force.

In recent years, after the advent of suitable computer facilities, some steps have been made to verify these ideas by numerical simulations. Getling (2001) and Getling & Ovchinnikov (2002) obtained numerical solutions to the three-dimensional nonlinear problem of magnetoconvection in a plane horizontal layer of an incompressible fluid, heated from below, and found that hexagonal convection cells interacting with a horizontal initial ("seed") magnetic field can produce various structures of the strongly amplified magnetic field, with a predominant bipolar component.

Correspondence to: A.Getling@ru.net
★ Present address: The University of Liverpool, Department of Mathematical Sciences, Applied Mathematics, Mathematics Building, Peach Street, Liverpool, L69 7ZL, UK.
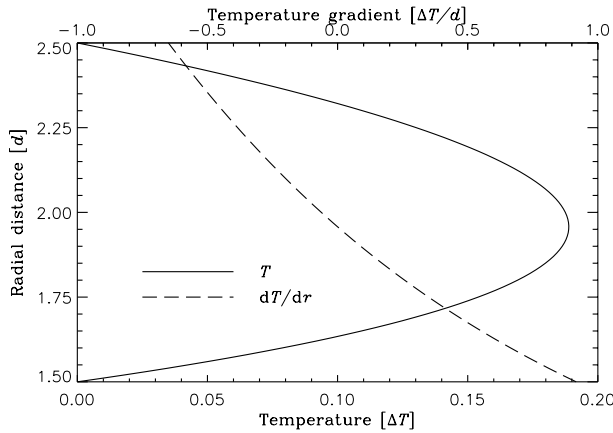
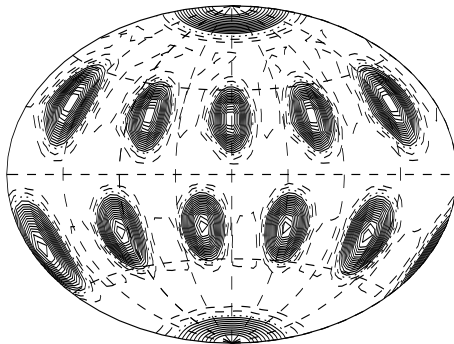**Fig. 1.** Static profiles of the temperature and temperature gradient.

Fig. 2. Contours of the radial component of the velocity on the sphere $r = r_i + 0.5$ at $t = 98.73$. Solid curves: positive values; dotted curves: zero values; dashed curves: negative values.

Dobler & Getling (2004) extended this numerical analysis to compressible fluids and obtained similar results.

Here, we numerically simulate a situation in which such a cellular dynamo can operate in a rotating spherical shell, with the final aim of comprehending to what degree the above-presented views may reflect the operation of the real solar dynamo. In our simulations, cellular magnetoconvection produces bipolar local magnetic configurations, which can in principle be associated with local manifestation of solar activity and which, in their subsequent evolution, ensure the re-generation of the poloidal field.

2. Formulation of the problem and numerical technique

We consider a spherical shell $r_i < r < r_o = r_i + d$ (with $\eta = r_i/r_o$ defined as a geometrical parameter of the problem) and assume that its inner and outer boundaries are stress-free, electrically insulating, and have perfect thermal conductivity. Thus, we can fix their temperatures T_i and T_o, respectively. We assume a Boussinesq approximation with a small quadratic term in the temperature dependence of density and specify internal heat sources distributed throughout the shell with a constant mass density q. Both the quadratic term and internal heating are introduced here since they favour the development of polygonal convection cells (instead of merid-
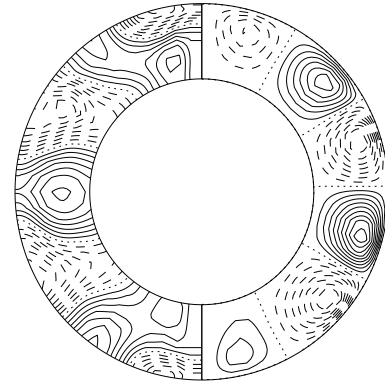

Fig. 3. Contours of the axisymmetric azimuthal velocity (left section) and streamlines of the meridional circulation, or contours of the stream function of the axisymmetric meridional flow (right section) at $t = 98.73$. The same notation as in Fig. 2 is used.

ionally stretched "bananas") similar to the cells observed on the Sun. Without these complicating factors, polygonal cells could only be obtained at much smaller rotational velocities; in this case, the process would develop very slowly, and the computations would be extremely time-consuming.

Under static conditions, the heat-transfer equation yields the following temperature distribution not perturbed by fluid motion (from here on, we measure the radial coordinate r in units of the shell thickness d):

$$T_s = \beta_0 - \frac{\beta}{2}d^2 r^2 + \frac{\beta_1}{d}\frac{1}{r}, \tag{1}$$

where $\beta = q/3\chi c_p$ (χ is the thermal diffusivity and c_p is the specific heat at constant pressure), $\beta_1 = \eta d\Delta T/(1-\eta)^2$, ΔT is the difference $T_i - T_o$ in the case of $q = 0$, and β_0 is a constant. In the general case, ΔT is related to the actual $T_i - T_o$ as follows:

$$\Delta T = T_i - T_o - \frac{1}{2}\beta d^2\frac{1+\eta}{1-\eta}. \tag{2}$$

The gravitational acceleration averaged over a spherical surface $r = \text{const}$ can be written as $\mathbf{g} = -\gamma\mathbf{r}$, where $\mathbf{r}$ is the position vector referenced to the centre of the spherical boundaries of the shell. The physical parameters of the problem are the Rayleigh numbers

$$R_i = \frac{\alpha\gamma\beta d^6}{\nu\chi}, \quad R_e = \frac{\alpha\gamma\Delta T d^4}{\nu\chi} \tag{3}$$

associated with the internal heating and the externally specified temperature difference (2), respectively (α is the volumetric coefficient of thermal expansion and ν is the kinematic viscosity), the Coriolis number, and the hydrodynamic and magnetic Prandtl numbers

$$\tau = \frac{2\Omega d^2}{\nu}, \quad P = \frac{\nu}{\chi}, \quad P_m = \frac{\nu}{\nu_m} \tag{4}$$

(Ω is the angular rotational velocity of the shell and ν_m is the magnetic viscosity). In addition to the above-described parameters, we specify a computational parameter — the fundamental (lowest nonzero) azimuthal number m_0; see below.
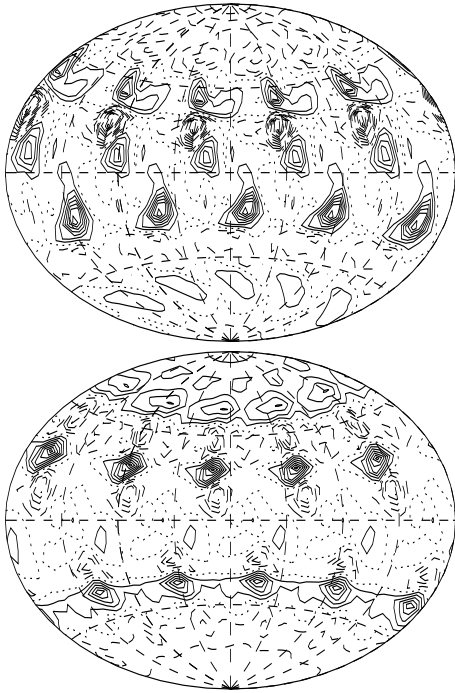
Fig. 4. Contours of the radial component of the magnetic field on the sphere $r = r_{\mathrm{o}} + 0.7$ at $t = 98.73$ (top) and 101.73 (bottom). The same notation as in Fig. 2 is used.
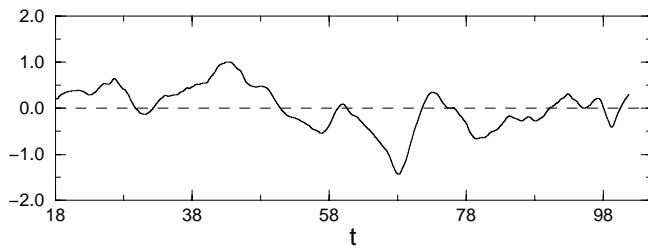

Fig. 5. Variation in the amplitude H_1^0 of the dipolar harmonic of the poloidal magnetic field at $r = r_{\mathrm{i}} + 0.5$.

The numerical simulations were carried out using the pseudospectral code developed by Tilgner and Busse (see Busse, Grote & Tilgner 1998; Tilgner 1999). In the computational algorithm, the solenoidal vector fields are represented in terms of toroidal and poloidal components; in particular, for the magnetic field,

$$\mathbf{B} = \nabla \times \mathbf{r}g + \nabla \times (\nabla \times \mathbf{r}h). \qquad (5)$$

The scalar fields are expanded into series in spherical harmonics $Y_l^m(\vartheta, \varphi) = P_l^m(\cos\vartheta)\,\mathrm{e}^{im\varphi}$ (where ϑ is the polar angle, φ is the azimuthal angle, and P_l^m are associated Legendre polynomials):

$$g = \frac{1}{r}\sum_{l=0}^{\infty}\sum_{m=-l}^{l} G_l^m(r,t) Y_l^m(\vartheta, \varphi), \qquad (6)$$

$$h = \frac{1}{r}\sum_{l=0}^{\infty}\sum_{m=-l}^{l} H_l^m(r,t) Y_l^m(\vartheta, \varphi), \qquad (7)$$

etc., with truncating the series at an appropriate maximum l. Finally, the radial dependences of the corresponding scalar

coefficients G_l^m, H_l^m, etc., are represented by (truncated) series in Chebyshev polynomials. Specifying the fundamental azimuthal number m_0 implies that only the following azimuthal harmonics are really considered:

$$1,\ \mathrm{e}^{\pm im_0\varphi},\ \mathrm{e}^{\pm 2im_0\varphi},\ \mathrm{e}^{\pm 3im_0\varphi}\ \ldots .$$

During the past several years, this code has been extensively (and highly successfully) employed to simulate planetary dynamos (see, e.g., Busse 2002; Simitev & Busse 2005).

3. Results

The case considered here is specified by the geometrical parameter $\eta = 0.6$, physical parameters $R_{\mathrm{i}} = 3000$, $R_{\mathrm{e}} = -6000$, $\tau = 10$, $P = 1$, $P_{\mathrm{m}} = 30$, and computational parameter $m_0 = 5$. The distributions of the temperature $T_{\mathrm{s}}(r)$ and its gradient $\mathrm{d}T_{\mathrm{s}}/\mathrm{d}r$ for the corresponding static-equilibrium state are shown in Fig. 1. Obviously, the outer part of the shell is convectively unstable and the inner part is stable.

The computations covered a time interval of about 100 in units of the time of thermal diffusion across the shell. During most part of this period, a very stable pattern of convection cells with a dodecahedral symmetry was observed (Fig. 2). No appreciable distortions due to the rotation of the shell can be noted in the cell shape. The entire pattern drifts in the retrograde direction, in agreement with theoretical predictions (Busse 2004).

A well-established flow pattern, nearly symmetric with respect to the equatorial plane, can also be seen in the axisymmetric component of the velocity field (Fig. 3). Specifically, a prograde rotation of the equatorial zone (in the frame of reference rotating together with the entire body) is present along with a retrograde rotation of the midlatitudes, and pairs of "secondary" prograde- and retrograde-rotation zones can also be noted in the polar regions. In a nonrotating frame of reference, the equatorial zone rotates more rapidly and the midlatitudinal zones more slowly than the shell as a whole does, and this pattern of differential rotation roughly resembles that observed on the Sun. Three meridional-circulation cells (pairs of vortices) fill the entire meridional section of the shell, from one pole to another.

The pattern of the magnetic field is less regular. One can hardly follow how the global toroidal field controls the formation of local fields amplified by the convection cells, nor can the process of regeneration of the global poloidal field be traced in detail. However, some remarkable features can be noted in the dynamo process, which is cyclic, although not quite regular.

1. Local magnetic-field configurations associated with convection cells arise repeatedly as bipolar magnetic regions (see Fig. 4 — the latitudinal belt of bipolar regions north of the equator in the upper plot and two such belts in the two hemispheres in the lower plot). In their subsequent evolution, these regions change their configuration and finally dissipate into much weaker remnant fields. In general outline, the pattern of bipolar regions is similar to the pattern of solar magnetic bipoles.
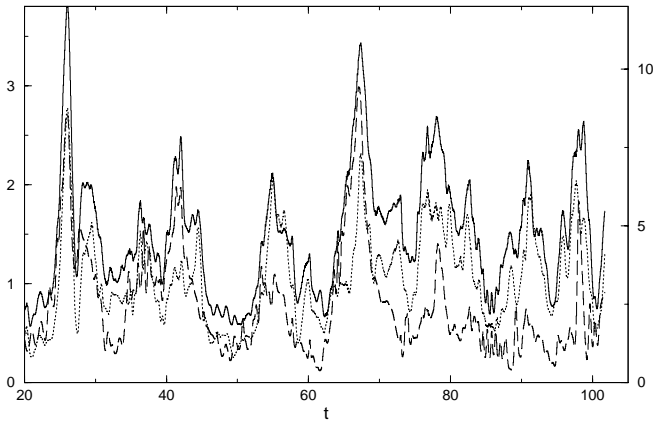
Fig. 6. Variations in the density of magnetic energy and in its particular fractions. Solid curve and right-hand scale: total density of the magnetic energy; dashed curve and left-hand scale: energy density associated with the axisymmetric part of the magnetic-field component that has a dipole symmetry; dotted curve and left-hand scale: energy density associated with the nonaxisymmetric part of the same magnetic-field component.

2. The dipolar component of the global magnetic field exhibits polarity reversals (Fig. 5). A reversal can be immediately observed if we follow the magnetic-field pattern in the polar regions. As can easily be seen, the two maps of the magnetic field shown in Fig. 4 correspond to situations in which the global magnetic dipole has opposite orientations (the polarity reversal between these two times corresponds to the rightmost intersection of the curve in Fig. 5 with the zero-amplitude abscissa). The magnetic polarities in the polar regions change when the "old" polarity is replaced by oncoming remnants of the magnetic regions, which have mainly the "new" polarity. Such poleward drift of the new polarity, which replaces the old one, also resembles the process actually observed on the Sun.

3. To reveal one more noteworthy feature of the computed scenario, let us consider the variations in the full magnetic energy of the system and in two particular fractions of the energy associated with the component of the magnetic field that has a dipole-type symmetry (i.e., is antisymmetric with respect to the equatorial plane). Specifically, we are interested in the behaviour of the energy of the axisymmetric and the nonaxisymmetric part of this magnetic-filed component. The axisymmetric part is represented by the spherical harmonics $H_1^0 Y_1^0$, $H_3^0 Y_3^0$, $H_5^0 Y_5^0$, ... , and the nonaxisymmetric part by other harmonics $H_l^m Y_l^m$ with $l + m$ odd. As can be seen from Fig. 6 (in which the total energy and its particular fractions are divided by the volume of the shell), the magnetic energy exhibits an intermittent behaviour. The main peaks in the graph of the total energy are alternately associated with increases in the energies of the axisymmetric and the nonaxisymmetric part of the magnetic-field component with a dipolar symmetry. In particular, the peak located near $t = 42$ is fed by the symmetric field; near $t = 55$, by the asymmetric

field; near $t = 68$, by both but with some predominance of the symmetric part; and near $t = 78$, again by the asymmetric part. To our knowledge, no counterpart to this phenomenon has been revealed on the Sun. From the standpoint of comprehending the properties of the real solar dynamo, it would be worth making corresponding comparisons for the global magnetic field of the Sun.

4. Concluding remarks

It is quite plausible that the α effect, in one form or another, is a fairly general property of various velocity fields that can maintain undamped regular magnetic fields. However, this property must not necessarily be associated with turbulent motion. In particular, the model velocity field in the toroidal eddies used by Getling & Tverskoy (1971) to construct a global dynamo included a rotational (with respect to the axis of the eddy) velocity component, so that the trajectories of the fluid particles were spirals deformed in a certain way. A similar property may also be inherent in the convective flow that develops in our computed scenario, although checking this possibility requires a special investigation.

At this stage, the "deterministic" cellular dynamo described here is oversimplified to be regarded as a model of the solar dynamo. However, it demonstrates that the dynamics of the well-structured local magnetic fields and of the global magnetic field may be ingredients of one complex process. Even if further studies show that the solar dynamo operates in ways quite different from that proposed in this paper, there is still the possibility that the magnetism of other stars could be generated in this way.

References

Busse, F.H.: 2002, PhFl 14, 1301
Busse, F.H.: 2004, Chaos 14, 803
Busse, F.H., Grote, E., Tilgner, A.: 1998, StGG 42, 211
Dobler, W., Getling, A.V.: 2004, in: A.V. Stepanov, E.E. Benevolenskaya, A.G. Kosovichev (eds.), *Multi-Wavelength Investigations of Solar Activity*, IAU Symp. 223, p. 239
Getling, A.V.: 2001, ARep 45, 569
Getling, A.V., Ovchinnikov, I.L.: 2002, ESA SP-506 2, 819 (Proc. of the 10th European Solar Physics Meeting, *Solar Variability: From Core to Outer Frontiers*)
Getling, A.V., Tverskoy, B.A.: 1971, Ge&Ae 11; 211, 389
Simitev, R., Busse, F.H.: 2005, JFM, in press
Tilgner, A.: 1999, Int. J. Num. Meth. in Fluids 30, 713
Tverskoy, B.A.: 1966, Ge&Ae 6, 11